

# Guidance Control and Docking of Remote Operated Vehicles

Xiang Li<sup>1</sup>, Yuichirou Toda<sup>1</sup>, Mamoru Minami<sup>1</sup>

<sup>1</sup>Okayama University, Japan  
(Tel: 81-86-251-8233, Fax: 81-86-251-8233)  
<sup>1</sup>pzk87r2@s.okayama-u.ac.jp

**Abstract:** Today, many robots are being researched and developed for various underwater tasks such as seabed exploration. Furthermore, research on autonomous underwater robot (AUV) is still in the developing stage and it can be said that it will become very important in the future. Currently, our research group is working on development of an automatic charging system based on visual servo technology for underwater robot which can perform various tasks such as automatic management of marine ranch, sea bottom search. However the measure of sailing to the working area and returning to the charging equipment have not been completed yet. In this paper, an automatic underwater simulation charging system for realizing the automatic control of underwater robot will be proposed. The system is using GPS measurement and guidance control method. And the usefulness of this automatic guidance system will be discussed by a repetition accuracy experiment and a guidance control experiment using mobile robot. Finally, the result of the newest simulated charging experiment in the actual sea of Okayama will be report.

**Keywords:** Underwater robot, GPS guidance, Automatic charging

## 1 INTRODUCTION

Recently, many studies have been performed worldwide to extend the persistence of underwater operations by autonomous underwater vehicles. Underwater battery recharging technology is one of the solutions even through challenges are still remained. The docking function takes place as an important role not only for battery recharging but also for other advanced applications such as intervention. Visual servoing in undersea environments inevitably encounters difficulties in recognizing the environment when captured images are disturbed by noise.

This study describes the effective recognition performance and robustness against air bubble disturbances in images captured by a real-time position and orientation (pose) tracking and servoing system using stereo vision for a visual-servoing-type underwater vehicle[1]. The recognition of the vehicle pose based on dynamic images captured by dual video cameras was performed by a real-time multi-step genetic algorithm (RM-GA)[2].

In previous studies[3], the docking performance was investigated under the condition that there were no disturbances in the captured images that address image degradation. And the robustness of the RM-GA against air bubble disturbances was verified through visual servoing and docking experiments in pool test to confirm that the system can continue to recognize the pose of the 3D marker and can maintain the desired pose by visual servoing. Then, the effectiveness of the proposed system against real disturbances such as turbidity that may degrade the visibility of the system in the sea was confirmed by conducting the docking experiment in a real sea, having verified the practicality of the pro-

posed method[4][5]. Based on the above motivation, some experiments were conducted to confirm the practicality of the proposed system against turbidity in the present paper.

In this study, three experiments were conducted in three different environments to assess the system performance in turbid environments and demonstrate the potential of the proposed system for real undersea applications. The recognition performance against different turbidity levels was verified first in a small pool. After this assessment of the recognition performance, the turbidity tolerance was verified by conducting docking experiments under different turbidity levels in a larger pool. Finally, a continuous iterative docking experiment was conducted in a shallow sea region near the town of Ushimado, Japan. Because this study focused on turbidity tolerance, a turbid coastal environment was selected over clear oceanic water to conduct the docking experiments.

Currently, our research group is working on development of an automatic charging system based on visual servo technology for underwater robot which can perform various tasks such as automatic management of marine ranch, sea bottom search. However the measure of sailing to the working area and returning to the charging equipment have not been completed yet.

In this paper, an automatic underwater simulation charging system for realizing the automatic control of underwater robot will be proposed. The system is using GPS measurement and guidance control method. And the usefulness of this automatic guidance system will be discussed by a repetition accuracy experiment and a guidance control experiment using mobile robot. Finally, the result of the simulated charging experiment in the sea of Okayama will be report.

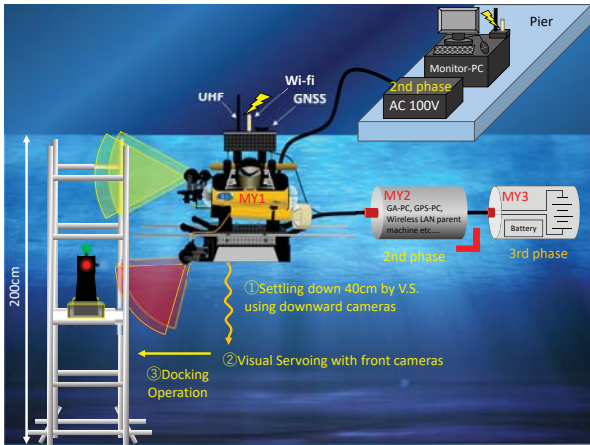


Fig. 1. Overview of underwater charging system

## 2 SYSTEM OVERVIEW

Fig.1 shows an overview of a simulated underwater auto-charging system combining visual servoing technology with GPS measurement and control. From Fig.1, development of this system is divided into three phases.

Phase 1: Realization of the simulated charging operation(docking). In order to realize the docking operation, two underwater cameras were mounted in front of the ROV for the real-time recognition of the 3D marker on the charging device (station) side. In this way, the ROV can obtain the relative position between itself and the station in real time to complete the docking operation.

Phase 2(current phase): Development of the automatic navigation system combining GPS and visual servoing technology. As shown in Fig.1(2nd phase), at this phase, the other two underwater cameras(downward), GPS receiver, geomagnetic sensor, pressure sensor and the will be mounted on the ROV. And some other control devices such as PC are stored in to a water resistant container(MY2 in Fig.1) which is towing behind the ROV. By using these sensors, this system can automatically navigate the ROV to the preset working area or help the ROV return to the charging device when the ROV is sailing on the sea.

Phase 3: Underwater charging experiment. A second traction type anti-pressure container(MY3 in Fig.1) will be added to the rear of the ROV, and the battery of ROV will be mounted in this container. And by combining the techniques used in the first two stages, to complete the development of the underwater charging system.

## 3 GPS AUTOMATIC NAVIGATION/HOMING CONTROL

Before installing the GPS measurement and control system into the ROV, we confirmed the positioning accuracy and

control effectiveness of the GPS receiver.

### 3.1 Repeatability Confirmation Experiment

In order to verify the operation confirmation of the RTK-GPS positioning equipment and the repetition accuracy of the positioning, we loaded the GPS receive(rover side) on a trolley, and repeated the homing experiment 100 times. As shown in Fig.2, the location of the repeatability confirmation experiment is the parking area in front of the 1st building of the Faculty of Engineering, Okayama University. The placement and the dimensions of the experimental are shown in Fig.2 and Fig.3. The antenna of the GPS base station was fixed at 2.1m from the ground and 1.8m away from the coordinate origin(docking end position). And the rover station of GPS is mounted on a trolley, the height of the antenna is 1.9m.

Flow of the experiment: 1, Place the rover station trolley at the initial position, and set this position as the coordinate origin(0, 0). 2, Move the rover station randomly and return to the predetermined position(0, 0), finally record the position of the rover station. 3, Repeat step-2 100 times to check the repetition accuracy.

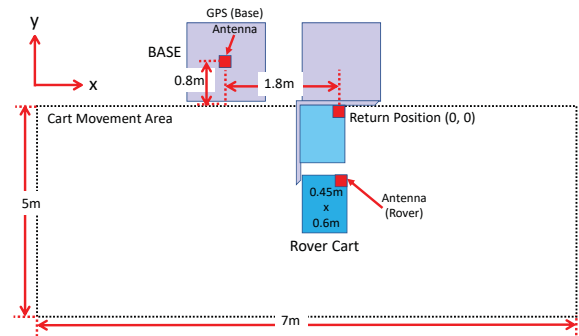


Fig. 2. Dimensions and layout of the experiment area

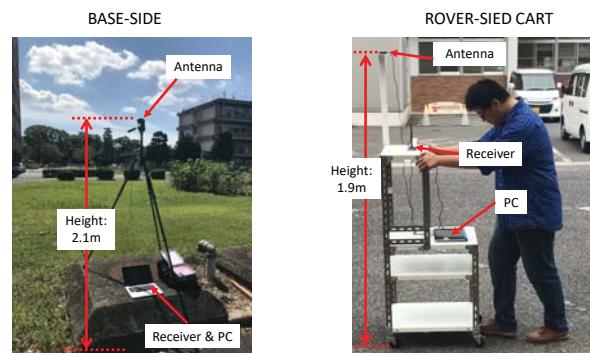


Fig. 3. Based side and rover side of GPS receiver

The results of experiment are shown in Fig.4 and Fig.5.

Fig.4 shows the measurement position when the mobile station carriage moves randomly and returns to the coordinate origin, and Fig.5 shows the approximate normal distribution curve of the deviation with respect to the X direction and the Y direction. From Fig.4, the distribution of position measurement results 100 times is within the range of  $\pm 30\text{mm}$  in the X direction, and  $\pm 40\text{mm}$  in the Y direction from the origin. Furthermore, as shown in Fig.5, the positioning error distribution in both X and Y directions has a probability of falling within 3 times the standard deviation ( $\pm 3\sigma$ ) is over than 99% , so the GPS positioning equipment has a good repetition accuracy.

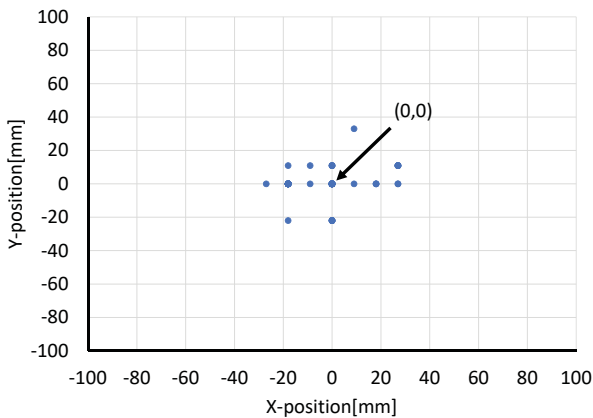


Fig. 4. Measurement position of GPS rover side receiver

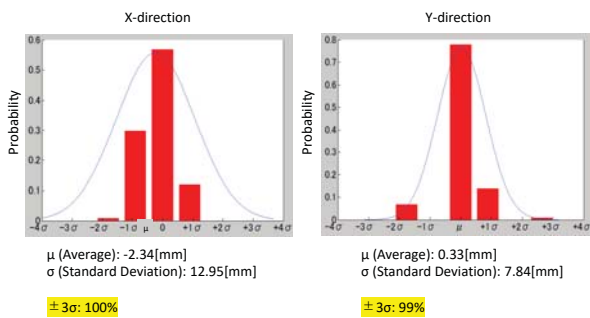


Fig. 5. Approximate normal distribution curve of deviation in x-direction and y-direction

### 3.2 Control Confirmation Experiment using Mobile Robot

In order to verify the effectiveness of the GPS control system, we installed a GPS receiver into a mobile robot shown in Fig.6, and carried out the guidance control experiment.

As shown in Fig.7, the location of this experiment is selected to the road in the north of the 11th building of the

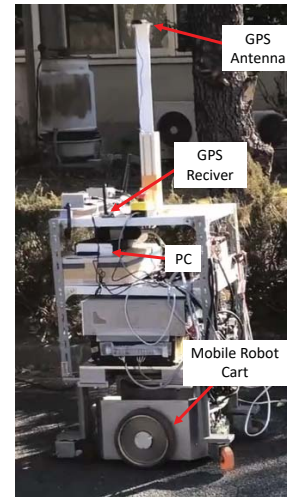


Fig. 6. Mobile robot with GPS receiver (rover side)

Faculty of Engineering, Okayama University. In the guidance control experiment, four target points and the target azimuth angle are specified in advance. And the mobile robot is guided to these target points by using GPS positioning data. The initial position and azimuth of the mobile robot is  $(x_0, y_0, \theta_0) = (0[m], 0[m], -1[^\circ])$ . And the target of the guidance control is  $(x_{d1}, y_{d1}, \theta_{d1}) = (2[m], 0[m], 90[^\circ])$ ,  $(x_{d2}, y_{d2}, \theta_{d2}) = (2[m], 2[m], 180[^\circ])$ ,  $(x_{d3}, y_{d3}, \theta_{d3}) = (0[m], 2[m], 270[^\circ])$ ,  $(x_{d4}, y_{d4}, \theta_{d4}) = (0[m], 0[m], 0[^\circ])$ . And the stopping condition is set to a distance deviation of less than 0.2m, and the angle deviation is less than  $2^\circ$ .



Fig. 7. Layout of the experiment area

Fig.8 shows the movement route of the mobile robot. As shown in Fig.8, the moving route of the mobile robot is like a square, and the position control deviation between the final stop position(0.092[m], 0.033[m]) and the start position(0[m], 0[m]) is within the assumed tolerance range(red dashed circle in Fig.8). So, we can indicate that the control system using the GPS positioning data is effective.

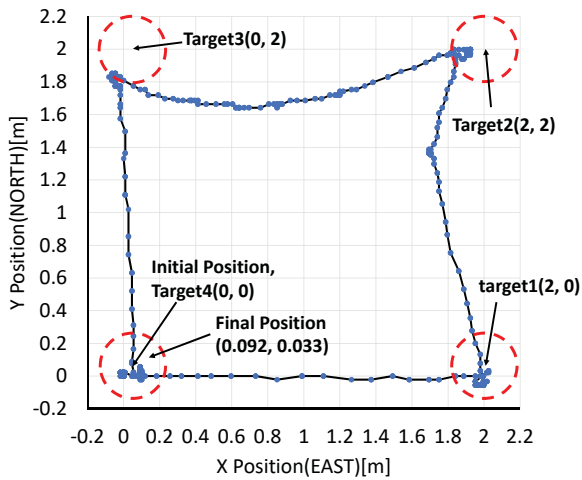


Fig. 8. Movement path of mobile robot (GPS measurement)

#### 4 SIMULATED CHARGING EXPERIMENT USING VISUAL SERVOING TECHNOLOGY

As the realization of the first phase of this system, the simulated charging experiment with the assuming of the ROV can return charging area by GPS guidance, and docking to the charging device by visual servoing control was performed on January 16, 2018, Ushimado, Okayama.

##### 4.1 Docking Condition

Fig.9 shows the flowchart about the docking condition of ROV. We move the ROV close to the target object(3D marker) manually until the target object displayed on the camera image. After confirming that the fitness value has risen to 0.2 or more, the control state will be switched to (a)Visual Servoing.

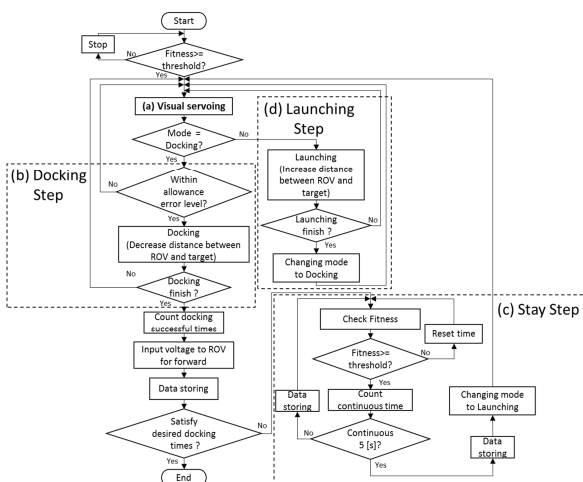


Fig. 9. Flow chart of ROV docking condition

##### (a)Visual Servoing

ROV finds the 3D marker and try to keep facing the 3D marker, the relative position/pose between the ROV and the marker will be kept at  $[x_d, y_d, z_d] = [600, 0, 0]$ [mm],  $\epsilon_d = [\epsilon_1, \epsilon_2, \epsilon_3] = [0, 0, 0]$ (in quaternion). Here,  $\epsilon_1, \epsilon_2$  are the pose of ROV around the X and Y axes, but they are stably maintained at 0 due to the relationship between the center of gravity and the buoyancy. When the ROV moving to the front of the 3D marker, and the tracking error in Y and Z axis less than 40[mm], and the error of  $\epsilon_3$  is less than 0.0615, and the ROV can keep this state longer than 165[ms], the control state will be switch to (b)Docking.

##### (b)Docking

The state of ROV go forward and try to docking to the charging device. When the ROV meet this conditions of  $|y_d - y| \leq 40$ [mm] and  $|z_d - z| \leq 40$ , we set the control target in X direction to  $x_d = 600 - 30t$ [mm](start time  $t = 0$ [s]) to make the ROV go forward with the speed of 30[mm/s] until the  $x_d$  reached the end value of 350[mm]. However, if the ROV cannot meet the docking condition, the control state will be returned to (a)Visual Servoing again.

##### (c)Stay

This state means the docking is completed. ROV will be order to keep a constant relative position and pose with the 3D marker( $[x_d, y_d, z_d] = [350, 0, 0]$ [mm],  $\epsilon_d = [\epsilon_1, \epsilon_2, \epsilon_3] = [0, 0, 0]$ ).

##### (d)Launching

Increase the control target of visual servoing in X direction to  $x_d = 600$ mm, make the ROV returns to the initial position.

#### 4.2 Results and Discussion

The results of the experiment are shown in Fig.10. In Fig.10, the dashed blue line indicates the target value(in the case of fitness, it shows the threshold), and the gray dashed line shows the range of the docking condition. As shown in Fig.10(A), the target value in the X direction decreases from 600mm to 350mm. And from Fig.10(B)(C)(D),  $y_d, z_d, \epsilon_3$  satisfies the docking condition(the target value  $y_d, z_d$  is between  $\pm 40$ [mm],  $\epsilon_3$  is between  $\pm 0.0615$  in 165[ms]) and the docking successful.

#### 5 CONCLUSION

In this paper, a charging system incorporating GPS measurement and guidance control for achieving AUV of under-

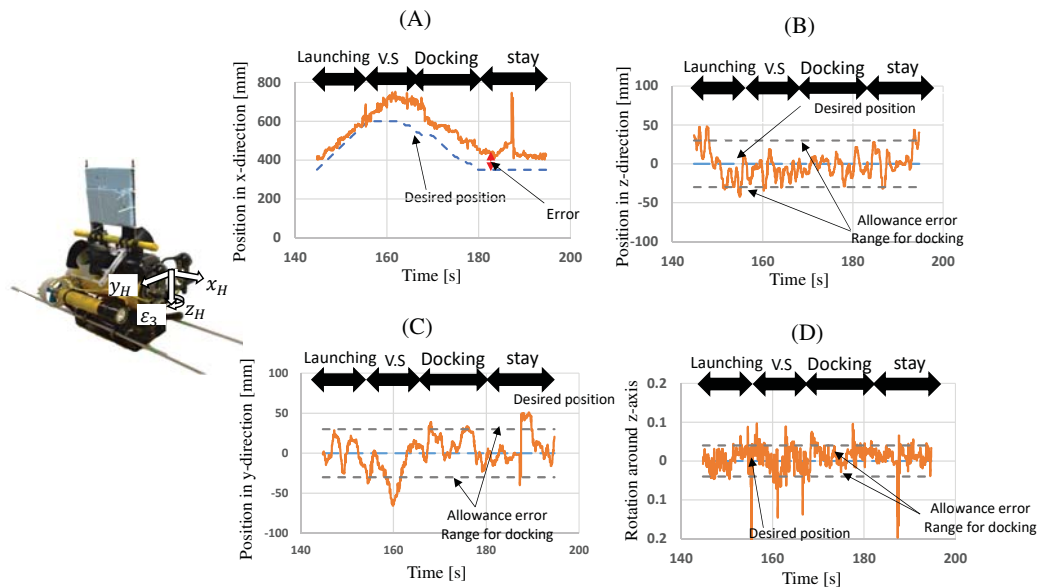


Fig. 10. Experimental results of simulated charging experiment. (A)Position in x-direction (B)Position in z-direction (C)Position in y-direction (D)Rotation around z-axis ( $\epsilon_3$ ).

water robot was proposed. And the usefulness of this system was confirmed by the repetition accuracy experiment, induction control experiment, and the simulated charging experiment conducted in the sea of Okayama.

## 6 ACKNOWLEDGMENT

The authors would like to thank Mitsui Engineering and Shipbuilding Co., Ltd.; and Kowa Corporation for their collaboration and support for this study.

## REFERENCES

- [1] Myo Myint, Kenta YONEMORI, Akira YANOU, Shintaro ISHIYAMA and Mamoru MINAMI, "Robustness of Visual-Servo against Air Bubble Disturbance of Underwater Vehicle System Using Three-Dimensional Marker and Dual-Eye Cameras", MTS/IEEE OCEANS, Washington, 18.Oct - 22.Oct, 2015.
- [2] Myo Myint, Kenta Yonemori, Akira Yanou, Khin Nwe Lwin, Mamoru Minami and Shintaro Ishiyama, "Visual-based Deep Sea Docking Simulation of Underwater Vehicle Using Dual-eyes Cameras with Lighting Adaptation", MTS/IEEE OCEANS ,Shanghai International Convention Center, April 10-13, 2016.
- [3] Khin Nwe Lwin, Myo Myint, Naoki Mukada, Daiki Yamada, Takayuki Matsuno, Mamoru Minami, "Docking Performance Against Turbidity Using Active Marker Under Day and Night Environment," 23rd International Symposium on Artificial Life and Robotics, B-Con Plaza Beppu, January 18-20, 2018.
- [4] Khin Nwe Lwin, Naoki Mukada, Myo Myint, Daiki Yamada, Mamoru Minami, Takayuki Matsuno, Kazuhiro Saitou, Waichiro Godou, "Docking at Pool and Sea by Using Active Marker in Turbid and Day/Night Environment", Artificial Life and Robotics, 2018.
- [5] Myo Myint, Kenta Yonemori, Khin New Lwin, Akira Yanou and Mamoru Minami, "Dual-eyes Vision-based Docking System for Autonomous Underwater Vehicle: An Approach and Experiments", Journal of Intelligent & Robotic Systems, 2017.